Chemistry Faculty Publications   Chemistry

2016

Development of Lithium Dimethyl Phosphate as an Electrolyte Additive for Lithium Ion Batteries

Mickdy S. Milien
University of Rhode Island

Usha Tottempudi
University of Rhode Island

Miyoung Son

Makoto Ue

Brett L. Lucht
University of Rhode Island, blucht@uri.edu

Development of Lithium Dimethyl Phosphate as an Electrolyte Additive for Lithium Ion Batteries

Mickdy S. Milien,[a,*] Usha Tottempudi,[a] Miyoung Son,[b] Makoto Ue,[b,**] and Brett L. Lucht[a,**,z]

[a]*Department of Chemistry, University of Rhode Island, Kingston, Rhode Island 02881, USA*
[b]*Battery R&D Center, Samsung SDI, 130 Samsung-ro, Yeongtong-gu, Suwon-si, Gyeonggi-do 443-803, South Korea*

The novel electrolyte additive lithium dimethyl phosphate (LiDMP) has been synthesized and characterized. Incorporation of LiDMP (0.1% wt) into $LiPF_6$ in ethylene carbonate (EC) / ethyl methyl carbonate (EMC) (3:7 wt) results in improved rate performance and reduced impedance for graphite / $LiNi_{1/3}Mn_{1/3}Co_{1/3}O_2$ cells. Ex-situ surface analysis of the electrodes suggests that incorporation of LiDMP results in a modification of the solid electrolyte interphase (SEI) on the anode. A decrease in the concentration of lithium alkyl carbonates and an increase in the concentration of lithium fluoro phosphates are observed. The change in the anode SEI structure is responsible for the increased rate performance and decreased cell impedance.

Lithium ion batteries (LIB) are currently the preferred source of power for consumer electronics such as mobile phones, computers, and cameras and are of interest for large-scale high-powered battery markets including aerospace, military, and electric vehicles. The reaction of non-aqueous electrolytes on the surface of the anode during the first few charging cycles results in the generation of a solid electrolyte interphase (SEI) which is critical to the performance of LIB.[1] While the structure and function of the anode SEI is still poorly understood, lithium ion intercalation through the SEI and into the anode is one of the largest limitations for high rate performance.[2–5]

Electrolyte additives have been used to modify the structure of the SEI and improve the performance of LIB via decreasing the irreversible capacity during formation, lowering SEI resistance, or stabilizing cells against extreme conditions such as high temperature and high rate cycling.[1,6–8] Vinylene carbonate (VC) is one of the most frequently investigated additives and has been used to generate a more stable SEI on graphite, but unfortunately the films are typically more resistive.[9] Improving the kinetics of lithium ion batteries has been investigated via incorporation of alternative co-solvents to improve electrolyte conductivity[10] or incorporation of electrolyte additives, such as propane sultone (PS), to reduce the impedance of the SEI.[11] Organophosphorus additives such as trimethyl phospshate and dimethylmethyl phosphonate have also been investigated as novel flame retarding additives.[12–14] Recently, a novel phosphorus additive, lithium difluoro phosphate (F_2PO_2Li), has been reported to improve the interfacial kinetics of the anode SEI.[15] In this manuscript, we report on the development of a structurally related novel organophosphorous additive, lithium dimethyl phosphate (LiDMP), which has been found to function as an anode film-forming additive, which decreases cell impedance.

Experimental

Materials.—All of the materials for the synthesis of LiDMP were purchased from Sigma Aldrich or Acros and used without further purification. Battery-grade ethylene carbonate (EC), ethyl methyl carbonate (EMC), and lithium hexafluorophosphate ($LiPF_6$) were provided by BASF, Germany, and used as received. LiDMP was washed and filtered 3 times and its purity was assessed from ^{1}H and ^{31}P NMR spectroscopy.

Synthesis of LiDMP.—Trimethyl phosphate 1.75 mL (14.9 mmol) was added, drop wise, to a solution of lithium iodide 2.00 g (14.9 mmol) in 100 mL of acetone and allowed to stir for 2 days in a nitrogen-filled glove box resulting in the generation of a precipatate.[16] The contents of the flask were filtered through a glass filter frit funnel to collect the precipitate. The precipitate was transferred to a round bottom flask, 15 mL of acetone was added, and the solution was allowed to stir for 2 hours to wash the crude product. The method above was repeated twice and the salt was dried over night under nitrogen on the schlenk line to yield LiDMP (1.76 g, white solid, 89% yield). ^{1}H NMR (300 MHz, D_2O): δ 3.54 (d, 6H, J = 27 Hz). ^{31}P NMR (300 MHz, D_2O): δ 2.98 (sept, J = 27 Hz).

Coin cell preparation.—Lithium ion coin cells containing an artificial graphite anode and a $LiNi_{1/3}Mn_{1/3}Co_{1/3}O_2$ cathode were prepared with 1.2 M $LiPF_6$ in EC: EMC (3:7 by volume, standard electrolyte, STD) with and without 0.1% (wt) added LiDMP. The negative electrodes were composed of 95.7% (wt) graphite, 3.8% (wt) carboxymethyl cellulose (CMC-SBR) binder, and 0.5% (wt) conductive carbon (Super P). The positive electrodes were composed of 93% (wt) $LiNi_{1/3}Mn_{1/3}Co_{1/3}O_2$, 4% (wt) polyvinylidene fluoride (PVDF) binder, and 3% (wt) conductive carbon. The coin cells were prepared with 105 µL electrolyte, 2 separators (a polyethylene film and a glass fiber).

Electrochemical testing.—Coin cells were cycled with a constant current-constant voltage charge and a constant current discharge between 4.2 V and 3.0 V using a battery cycler (BT-2000 Arbin cycler, College Station, TX). The cells were cycled with the following formation procedure: first cycle at C/20, D/20, second and third cycles at C/10, D/10, and the fourth and fifth cycles at C/5, D/5. After the initial five formation cycles the cells were cycled at a C/5, D/5 rate for 15 cycles at room temperature, followed by 3 cycles each of C/3, D/3, C/2, D/2, C, D, 2C, 2D, 3C, 3D, 5C, 5D, and C/5, D/5, respectively.

All cells were prepared in duplicate to confirm reproducibility of the cycling behavior. Additional cells were prepared to optimize LiDMP concentration and similar results were obtained. Representative cycling data are presented. After 20 cycles, electrochemical impedance spectroscopy (EIS) was measured at a 0% state of charge on a Solartron SI 1287 electrochemical interface and SI 1252A

*Electrochemical Society Student Member.
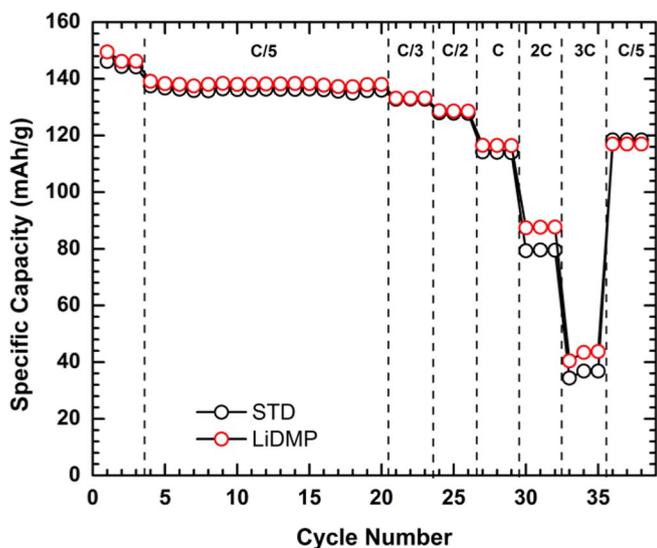**Electrochemical Society Member.
zE-mail: blucht@chm.uri.edu

Figure 1. Cycling retention and rate performance of $LiNi_{1/3}Co_{1/3}Mn_{1/3}O_2$/Graphite cells at 25°C with the baseline electrolyte (STD) and with the baseline + LiDMP.

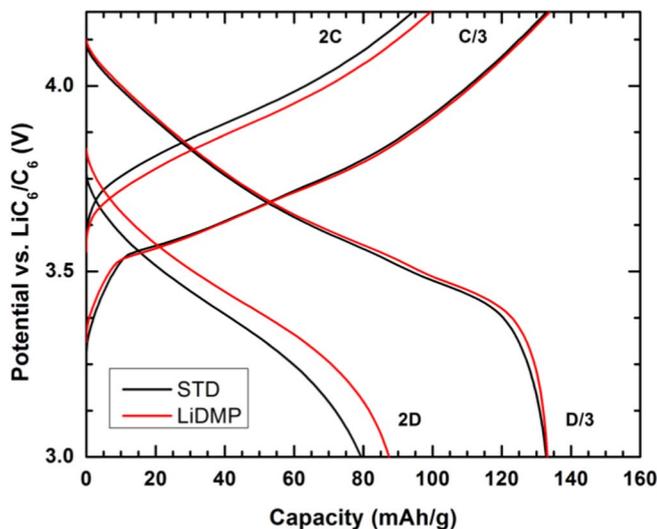**Figure 2.** Voltage profile of $LiNi_{1/3}Co_{1/3}Mn_{1/3}O_2$/Graphite cells at 25°C (C/3, D/3, 2C, and 2D between 3.0V and 4.2V) with the baseline electrolyte (STD) and the baseline + LiDMP.

frequency response analyzer with an AC perturbation of 10 mV and frequency range of 300 kHz - 30 mHz. Cells were then cycled at elevated rates, allowed to rest in order to obtain equilibrium, and EIS measurements were repeated.

In order to measure the impedance of symmetrical graphite and symmetrical NCM 111 cells, 4 cells containing the standard electrolyte were assembled using the method previously mentioned. The cells were charged to 4.2 V, allowed to rest, and opened. The electrodes were harvested and 2 symmetrical lithiated graphite cells as well as 2 symmetrical delithiated NCM111 cells were assembled in the method previously mentioned, allowed to rest in order to obtain equilibrium, and analyzed in-situ via EIS using the parameters previously mentioned. Symmetric cells were prepared from electrodes cycled with standard electrolyte with and without added LiDMP.

Ex-situ surface analysis.—The cells were disassembled in an argon glove box. The electrodes were rinsed with dimethyl carbonate (DMC) three times to remove residual EC and $LiPF_6$ and evacuated overnight prior to surface analysis. X-ray photoelectron spectroscopy (XPS) was acquired with a Thermo K-alpha system using Al Kα radiation (hυ = 1486.6 eV) under ultra high vacuum and a measured spot size of 400 μm. Samples were transferred into the XPS chamber with a vacuum transfer vessel. The binding energy was corrected based on the C 1s of C-C at 284.3 eV. The spectra obtained were analyzed using Thermo Advantage software (version 5.926). A mixture of 30% Laurentzian and 70% Gaussian functions was used for the least-squares curves fitting procedure.

Results and Discussion

Electrochemical testing.—A comparative study of $LiNi_{1/3}Mn_{1/3}Co_{1/3}O_2$/Graphite cells with the standard electrolyte and the standard electrolyte with 0.1% (wt) of added LiDMP was conducted in order to assay the effect of the additive on cycling behavior. Capacity retention and rate performance of cells cycled with and without LiDMP are displayed in Figure 1. Although both sets of cells display similar capacity retention at low rates, cells cycled with LiDMP exhibit a higher first cycle coulombic efficiency (CE) of 91.5% compared to 87.9% of cells cycled with the standard electrolyte. The improved rate performance of the standard electrolyte with added LiDMP at 2C and 3C suggests that there is less resistance, with LiDMP.

The voltage profile of the NCM111/Graphite cells at C/3 and 2C are displayed in Figure 2. The cell with added LiDMP has comparable capacity to the cell with the standard electrolyte at C/3 and significantly more capacity at 2C. The larger voltage hysteresis observed for the cell cycled with standard electrolyte provides further support
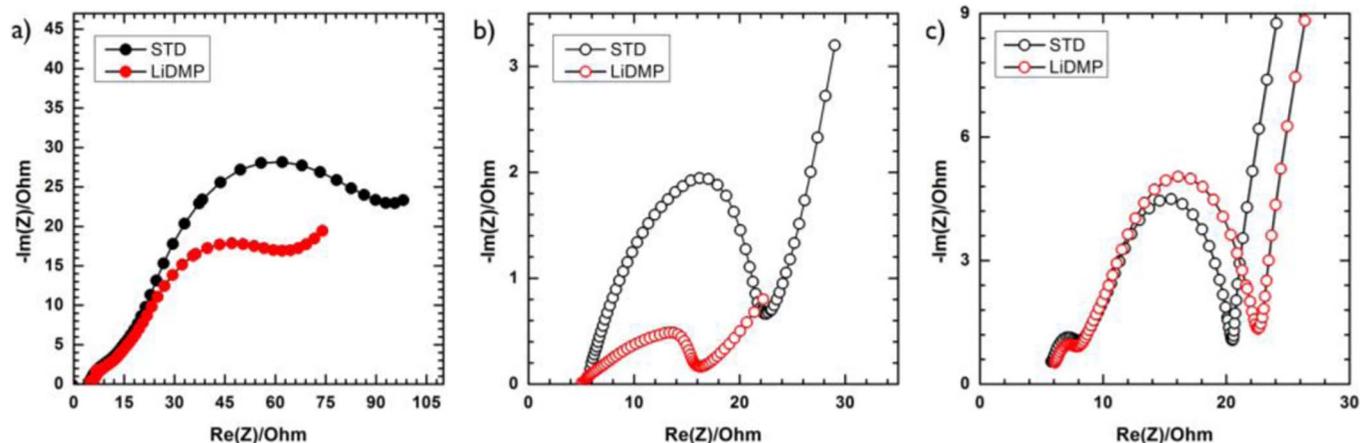

Figure 3. EIS measurements at OCV of a) $LiNi_{1/3}Co_{1/3}Mn_{1/3}O_2$/Graphite cells which have undergone formation cycling at 25°C (0% SOC), b) Symmetrical lithiated graphite cells, and c) Symmetrical delithiated NCM111.
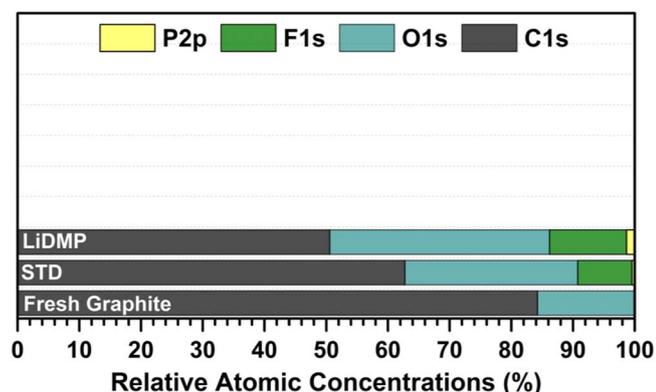
Figure 4. Relative atomic concentrations of elements detected on the surface of the fresh anode, the anode which has undergone formation cycling at 25°C with the baseline electrolyte, and the anode which has undergone formation cycling with the baseline electrolyte + LiDMP.

for reduced cell resistance with added LiDMP. The passivation film generated for the cell cycled with LiDMP is more conductive than that generated without LiDMP. This is demonstrated by the decrease in ohmic potential drop observed in the 2D discharge curve in Figure 2 of the cell cycled with 0.1% (wt) LiDMP

Impedance measurements of the NCM111/Graphite cells, which have undergone formation at 25°C, with and without LiDMP, are displayed in Figure 3a. The cells cycled with added LiDMP have lower impedance than the cells cycled with the standard electrolyte, consistent with the rate data. Again, this is attributed to the LiDMP-derived surface film, which improves charge-transfer. In order to determine whether the improved resistance is due to changes with the the anode or the cathode, symmetrical cells of lithiated graphite and delithiated NCM111 were constructed. The impedance measurements of the symmetrical cells are displayed in Figures 3b and 3c, respectively. The graphite symmetrical cell with added LiDMP has significantly less resistance than the graphite symmetrical cell with the standard electrolyte (Figure 3b) while the NCM111 symmetrical cells have similar impedance with and without added LiDMP (Figure 3c), this

demonstrates that the reduced resistance is a function of the LiDMP modifying the SEI on the anode.

Surface characterization.—The relative atomic concentrations of elements detected on the surface of fresh graphite electrodes and graphite electrodes extracted from cells which have undergone formation cycling at 25°C with the standard electrolyte (STD) and STD with added LiDMP are shown in Figure 4. The electrode cycled with the standard electrolyte has an increase in the concentration of O, F and P, and a decrease in the concentration of C, supporting the generation of an SEI on the surface of the active material. Similar results are observed for the cell cycled with the electrolyte with added LiDMP except there is a greater increase in the concentrations of O, F, and P, and a greater decrease in the concentration of C, which suggests a structural modification of the SEI upon incorporation of LiDMP.

The C1s XPS spectra of fresh graphite electrode and the graphite electrodes cycled with the standard electrolyte with and without added LiDMP are displayed in Figure 5. A decrease in the intensity of the C-C peak (284.3 eV) combined with the increases in the intensity of the C-H (285.6 eV), C-O (286.0 eV), CO_2 (288.1 eV), and CO_3 (290.1 eV) peaks indicates that an organic passivation layer generated from the reduction of EC covers the graphite electrode.[3] Related peaks associated with C-H, C-O, and CO_3 are observed on the surface of the electrode cycled with added LiDMP, but the intensity of the new absorptions are weaker, consistent with less EC reduction on the anode surface.

The F1s XPS spectra are very similar for both the electrode cycled with the standard electrolyte and the electrode cycled with added LiDMP. Small amounts of $Li_xPO_yF_z$ (687.2 eV) and larger amounts of LiF (685.0 eV) are present on the surface of both electrodes. The O1s XPS spectra differ in that the electrode cycled with LiDMP displays small amounts of Li_2O (528.8 eV), significantly less C-O species (533.0 eV), and a significantly greater peak at 531.6 eV, which corresponds to the binding energy of Li_3PO_4.[17]

The P2p XPS spectra of the electrode cycled with the standard electrolyte with and without added LiDMP are provided in Figure 5. The electrode cycled with the standard electrolyte has a low concentration of residual $LiPF_6$ and/or $Li_xPO_yF_z$ at 138.0 eV and low concentration of phosphates at 134.0 eV. The electrode cycled with electrolyte containing added LiDMP also has a low concentration of $LiPF_6$ and/or $Li_xPO_yF_z$, but the concentration of phosphates are
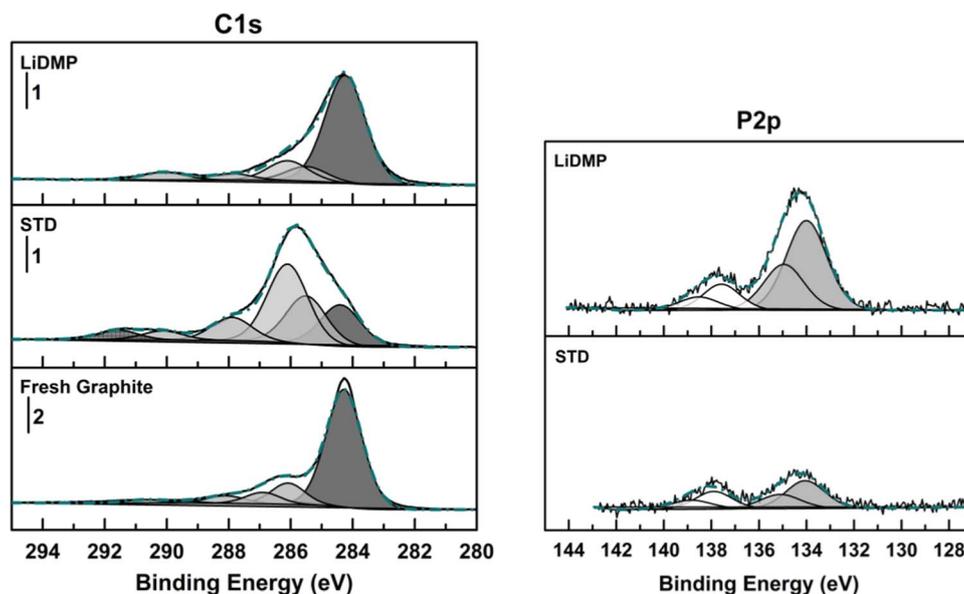

Figure 5. C1s core spectra of fresh graphite, graphite which has undergone formation at 25°C with the baseline electrolyte, and graphite which has undergone formation with the baseline electrolyte + LiDMP (left). P2p core spectra of graphite which has undergone formation at 25°C with the baseline electrolyte and graphite which has undergone formation with the baseline electrolyte + LiDMP (right).

significantly greater, consistent with deposition of LiDMP reduction products on the surface of the anode. The increased concentration of phosphates likely correlates with the reduced impedance of the cycled anodes. Similar observations have been observed with other additives that generate phosphate or sulfate rich SEIs.[15,18]

Conclusions

The novel lithium salt, lithium dimethyl phosphate (LiDMP), was synthesized and investigated as an anode film forming electrolyte additive. Incorporation of LiDMP into a standard electrolyte formulation results in improved first cycle efficiency, improved rate performance and decreased cell impedance on the graphitic anode. Ex-situ surface analysis of the cycled anodes reveals lower concentrations of lithium alkyl carbonates, consistent with the improved efficiency, and a higher concentration $Li_xPO_yF_z$ on electrodes cycled with added LiDMP. Thus reduction of LiDMP results in higher concentrations of ionically conductive $Li_xPO_yF_z$ in the anode SEI and reduces cell impedance.[15] Similar improvements have been reported for additives which result in the generation of phosphate or sulfate rich SEIs.

Acknowledgment

References

1. K. Xu, *Chem. Rev.*, **114**, 11503 (2014).
2. P. Verma, P. Maire, and P. Novak, *Electrochim. Acta.*, **55**, 6332 (2010).
3. M. Nie, D. Chalasani, D. P. Abraham, Y. Chen, A. Bose, and B. L. Lucht, *J. Phys. Chem. C*, **117**, 1257 (2013).
4. F. Puglia, R. Gitzendanner, C. Marsh, and T. Curran, *J. Power Sources*, **96**, 40 (2001).
5. Y. Yamada, Y. Iriyama, T. Abe, and Z. Ogumi, *Langmuir*, **25**, 12766 (2009).
6. K. Zaghib, M. Dontigny, A. Guerfi, P. Charest, I. Rodrigues, A. Mauger, and C. M. Julien, *J. Power Sources*, **196**, 3949 (2011).
7. H. W. Rollins, M. K. Harrup, E. J. Dufek et al. *J. Power Sources*, **263**, 66 (2014).
8. S. Menkin, D. Golodnitsky, and E. Peled, *Electrochem. Commun.*, **11**, 1789 (2009).
9. Y. Qin, Z. Chen, J. Liu, and K. Amine, *Electrochemical and Solid-State Letters*, **13**, A11 (2010).
10. M. C. Smart, B. V. Ratnakumar, K. B. Chin, and L. D. Whitcanack, *J. Electrochem. Soc.*, **157**(12), A1361 (2010).
11. M. Q. Xu, W. S. Li, and B. L. Lucht, *J. Power Sources*, **193**, 804 (2009).
12. J. Feng, P. Ma, H. Yang, and L. Lu, *Electrochim. Acta.*, **114**, 688 (2013).
13. S. Dalavi, M. Xu, L. Zhou, B. Ravdel, and B. L. Lucht, *J. Electrochem. Soc.*, **157**, A1113 (2010).
14. K. Xu, M. S. Ding, S. Zhang, J. L. Allen, and T. R. Jow, *J. Electrochem. Soc.*, **150**, A161 (2003).
15. K.-E. Kim, J. Y. Jang, I. Park, M.-H. Woo, M.-H. Jeong, W. C. Shin, M. Ue, and N.-S. Choi *Electrochm. Comm.*, **61**, 121 (2015).
16. M. Mentz, A. M. Modro, and T. A. Modro, *J. Chem. Research (S)*, 1, 46 (1994).
17. A. C. Kozen, A. J. Pearse, C. Fu, M. Noked, and G. W. Rubloff, *Chem. Mater.*, **27**, 5324 (2015).
18. B. Zhang, M. Metzger, S. Solchenbach, M. Payne, S. Meini, H. Gasteiger, A. Garsuch, and B. L. Lucht, *J. Phys. Chem. C.*, **119**, 11337 (2015).